

# Understanding Rapid Evolution in Predator-Prey Interactions Using the Theory of Fast-Slow Dynamical Systems

Michael H. Cortez<sup>1,\*</sup> and Stephen P. Ellner<sup>1,2</sup>

1. Center for Applied Mathematics, Cornell University, Ithaca, New York 14853; 2. Department of Ecology and Evolutionary Biology, Cornell University, Ithaca, New York 14853

Submitted November 17, 2009; Accepted June 5, 2010; Electronically published September 23, 2010

Online enhancements: appendixes.

**ABSTRACT:** The accumulation of evidence that ecologically important traits often evolve at the same time and rate as ecological dynamics (e.g., changes in species' abundances or spatial distributions) has outpaced theory describing the interplay between ecological and evolutionary processes with comparable timescales. The disparity between experiment and theory is partially due to the high dimensionality of models that include both evolutionary and ecological dynamics. Here we show how the theory of fast-slow dynamical systems can be used to reduce model dimension, and we use that body of theory to study a general predator-prey system exhibiting fast evolution in either the predator or the prey. Our approach yields graphical methods with predictive power about when new and unique dynamics (e.g., completely out-of-phase oscillations and cryptic dynamics) can arise in ecological systems exhibiting fast evolution. In addition, we derive analytical expressions for determining when such behavior arises and how evolution affects qualitative properties of the ecological dynamics. Finally, while the theory requires a separation of timescales between the ecological and evolutionary processes, our approach yields insight into systems where the rates of those processes are comparable and thus is a step toward creating a general ecoevolutionary theory.

**Keywords:** coevolution, ecoevolutionary dynamics, predator-prey, fast-slow dynamics.

## Introduction

Over the past 30 years, the evolution of ecologically important species' traits at ecological rates (ecoevolutionary dynamics: Fussmann et al. 2007; Kinnison and Hairston 2007) has been observed in species of algae (Yoshida et al. 2003), bacteria (Bohannan and Lenski 2000; Palumbi 2001), birds (Grant and Grant 2002), crustaceans (Hairston and Walton 1986; Hairston and Dillon 1990; Hairston et al. 1999), fishes (Reznick et al. 1997, 2008; Conover and Munch 2002; Heath et al. 2003; Swain et al. 2007; Kinnison

et al. 2008), mammals (Pelletier et al. 2007), and reptiles (Sinervo et al. 2000). Predator-prey and other exploiter-victim systems are important examples where ecoevolutionary dynamics have been observed. Changes in prey phenotypes can help the prey avoid encounters with predators (Hairston and Walton 1986; Hairston and Dillon 1990; Reznick et al. 1997, 2008; Heath et al. 2003) or defend against attacks (Bohannan and Lenski 2000; Yoshida et al. 2003; Jones et al. 2009), while consumer evolution can allow for increased resource capture and consumption (Grant and Grant 2002) and the ability to overcome prey defenses (Hairston et al. 1999). Furthermore, genetic variation among individuals can have strong effects on observed community-level dynamics (Post and Palkovacs 1997; Tuda 1998; Hanski and Saccheri 2006; Saccheri and Hanski 2006; Bailey et al. 2009; Ezard et al. 2009; Johnson et al. 2009; Palkovacs et al. 2009).

These studies yield two complementary results. First, one can no longer assume that ecologically important traits are fixed on the timescale of ecological dynamics such as changes in the abundance, structure, or distribution of populations. Second, heritable changes in phenotype that occur at the same rate as ecological processes can influence the ecological interactions that cause them. These two observations emphasize the need to understand heritable changes within a population that occur fast enough to affect interspecific interactions while they are still taking place and also how they can change observable community-level patterns.

Recent studies have begun to develop theory to account for the interplay between ecological and evolutionary processes with comparable timescales in predator-prey systems. By comparable timescales, we mean that change of organismal traits occurs at the same time and pace as ecological dynamics. Most studies have focused on the qualitative and quantitative changes in population dynamics resulting from rapid evolution, but largely with models tailored to specific systems (Abrams 1992; Abrams and Matsuda 1997a, 1997b; Yoshida et al. 2003, 2004; Jones et

\* Corresponding author; e-mail: mhc37@cornell.edu.

Am. Nat. 2010. Vol. 176, pp. E109–E127. © 2010 by The University of Chicago. 0003-0147/2010/17605-51737\$15.00. All rights reserved.  
DOI: 10.1086/656485

al. 2009). While these studies have yielded qualitatively new population dynamics, the studies may not exhibit all possible ecoevolutionary dynamics, and consequently, new or unique dynamics can be missed. Furthermore, with only a few specific examples it is often difficult to determine the general biological and mathematical mechanisms that cause the new dynamical behavior to arise. Hence, we believe a more general theory is needed in order to characterize the full spectrum of dynamics that ecoevolutionary systems can exhibit.

An inherent difficulty in studying systems with rapid evolution is the intractability of higher (three or more)-dimensional systems. Even simple predator-prey ecoevolutionary systems are difficult to understand since they must be of at least three dimensions. To begin developing a generalized ecoevolutionary theory and to reduce model dimension, we start with an analytically tractable case where the evolution of a species occurs much faster than do changes in population size. This separation of time-scales is the opposite of that assumed in traditional theory but is not biologically ill-founded. Such a case can arise if there is a rapid turnover of individuals in a population and the birth rate is nearly equal to the death rate (e.g., if the population is space limited and close to its carrying capacity). In this case, the average trait value of the population changes quickly while the total population size changes slowly.

Another justification for considering the fast-evolution limit is that increasing the rate of evolution often preserves some of the main qualitative properties of the dynamics observed in systems where the ecological and evolutionary processes have comparable rates. Figure 1A presents data from an experimental algal-rotifer system (Fussmann et al. 2000) where prey evolution has been shown to affect qualitative properties of the predator-prey oscillations (Yoshida et al. 2003, 2007; Meyer et al. 2006). Figure 1B–1D contains time series from a model fitted with data that predict the dynamics of the algal-rotifer system (Jones and Ellner 2007). In figure 1B with parameters estimated from experimental data, the evolutionary changes and population changes of the model occur on the same timescale. As the evolutionary processes are sped up by a factor of 5 (fig. 1C) or by a factor of 10 (fig. 1D), the essential qualitative properties of the dynamics do not change. In particular, the completely out-of-phase predator-prey oscillations in the data are preserved as the speed of evolution is increased in the model.

Figure 1 emphasizes a key point underlying our fast-evolution approach. When we speed up the evolutionary processes we are not positing that evolution can occur at instantaneous rates. Rather, we study the dynamics that occur in the fast-evolution limit because these dynamics yield insight into the behavior exhibited by systems where

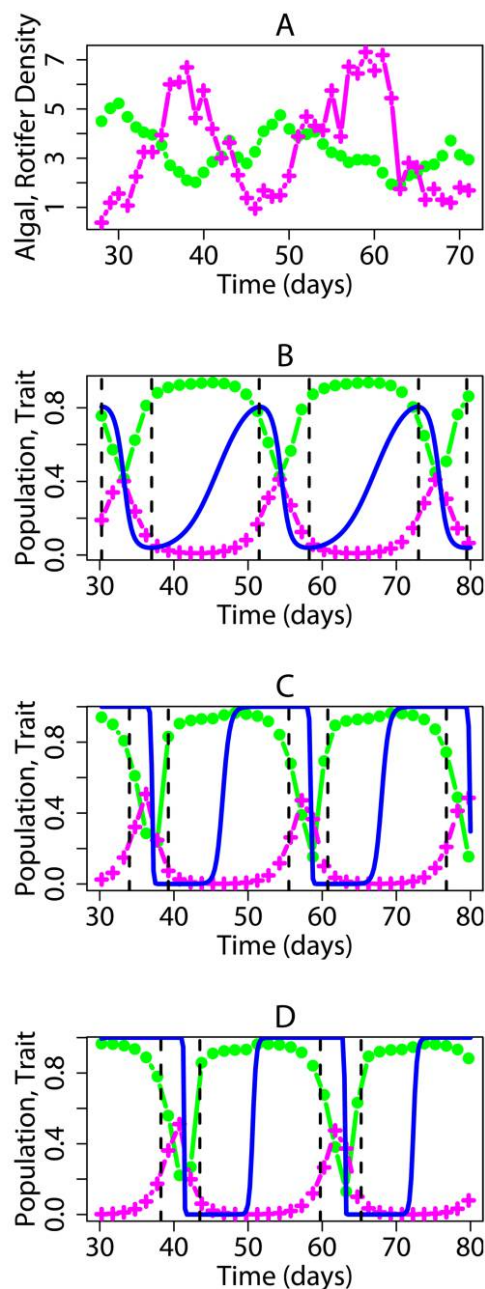


**Figure 1:** Comparison of experimental and theoretical results for a predator-prey system as evolution is sped up. A, Algal (*Chlorella vulgaris*, green circles) and rotifer (*Brachionus calyciflorus*, magenta plus signs) density data from Fussmann et al. (2000). Units are  $10^6$  cells  $\text{mL}^{-1}$  (algae) and number of females  $\text{mL}^{-1}$  (rotifers). B–D, Predator (magenta plus signs), prey (green circles), and trait (blue lines) time series for a predator-prey model with prey evolution (Jones and Ellner 2007). Speed of evolution: as fast as the ecological dynamics (B); five times as fast (C); and 10 times as fast (D). The black dashed lines denote when the direction of selection switches in the model. The trait values are rescaled such that the minimum value corresponds to 0 and the maximum value corresponds to 1.

the ecological and evolutionary processes have comparable rates. In figure 1, when the speed of evolution is increased, the ecoevolutionary dynamics do not become increasingly complicated, nor do they become increasingly unrealistic. Thus, by considering this extreme in evolutionary rates we can begin to develop a general ecoevolutionary theory.

We note that the opposite limit, where evolutionary processes are much slower than ecological processes, has been studied elsewhere in the literature (e.g., Khibnik and Kondrashov 1997; Dercole et al. 2006). While the slow-evolution viewpoint yields insight into the effects ecological processes have on evolutionary dynamics, our approach yields insight into the effects evolutionary processes have on ecological dynamics. Furthermore, the slow-evolution limit does not predict or capture all experimentally observed population dynamics (e.g., the completely out-of-phase oscillations in fig. 1A). Since the fast-evolution limit does yield insight into this behavior, our approach complements the traditional viewpoint, and together these extremes can be used to understand systems where ecological and evolutionary rates are comparable.

Figure 1 also demonstrates why it is not sufficient to study systems with inducible defenses (e.g., see Vos et al. 2004) to understand the dynamics in systems with fast evolution. As the speed of evolution increases in figure 1, a lag between the switch in the direction of selection (*vertical black lines*) and a corresponding measurable change in the trait arise. This lag in the trait is not observed in ecological models with induced defenses, and due to its influence on population dynamics, it distinguishes ecological models with fast evolution from ones with induced defenses.

Mathematically, an ecoevolutionary model exhibiting fast evolution is a fast-slow dynamical system, an area known as singular perturbation theory (Arnold et al. 1995). This body of theory allows one to study dynamical systems where there is a separation of timescales and some variables change much faster than others. The theory focuses on the limit where the fast variables are instantaneously fast so as to reduce the complexity of the mathematics. In this study, we use fast-slow systems theory to study the effects of fast evolution in a single species on the ecological dynamics of a general predator-prey system. In our model, predator and prey evolution are nearly mathematically equivalent by a reversal of time. Consequently, we will present our results for the predator evolution case and discuss the differences that arise between the two.

In the next section, we use a familiar predator-prey model to introduce the basic concepts of slow-fast systems theory, and we then present our general predator-prey model with rapid predator evolution. The results section begins with two consequences of predator evolution: how

the addition of fast evolution to an ecological system can stabilize or destabilize population dynamics and how the trait's trade-off curve influences population and trait time series. We then present a simple graphical technique that predicts the full spectra of possible population dynamics for systems with particular types of evolutionary dynamics. The last section of "Results" deals with the differences between predator and prey evolution.

### Fast-Slow Systems and Models

To introduce some basic concepts of fast-slow dynamical systems we consider a modified Rosenzweig-MacArthur model (Rosenzweig and MacArthur 1963). We assume that the prey responds to ecological conditions faster than the predator does. Such a case would be analogous to thinking about birds (long lifetimes) and their insect prey (shorter lifetimes). Our model is

$$\begin{aligned}\epsilon \frac{dx}{dt} &= x \left( r - \frac{x}{K} - \frac{ay}{1 + hx} \right), \\ \frac{dy}{dt} &= y \left( \frac{bay}{1 + hx} - d \right),\end{aligned}\quad (1)$$

where  $x$  is prey density,  $y$  is predator density,  $r$  is the exponential growth rate of the prey without density limitation,  $K$  is the prey carrying capacity,  $a$  is the encounter rate,  $h$  is the handling time,  $b$  is the conversion of prey to predator density, and  $d$  is the per capita death rate of the predator. In this model,  $\epsilon$  is a small positive number that represents the difference in timescales between the prey and predator species. It is meant to explicitly flag that the prey population processes are occurring on a faster timescale than the predator processes.

Solutions to a fast-slow system, as in figure 2B, behave in a way that is qualitatively different from models without a separation of timescales (fig. 2A). In particular, solutions of such a system spend nearly all of their time near an object called the critical manifold and the rest jumping between different pieces of the critical manifold. For a general fast-slow system, the critical manifold,  $C$ , is the set of equilibria of the fast variable when  $\epsilon = 0$  and the slow variables are held constant. These points make up a collection of curves or planes in the full system. In system (1),  $C$  is the set of points satisfying  $dx/dt = 0$ , or equivalently, the predator axis and prey nullcline:

$$C = \left\{ (x, y) : x \left( r - \frac{x}{K} - \frac{ay}{1 + hx} \right) = 0 \right\}. \quad (2)$$

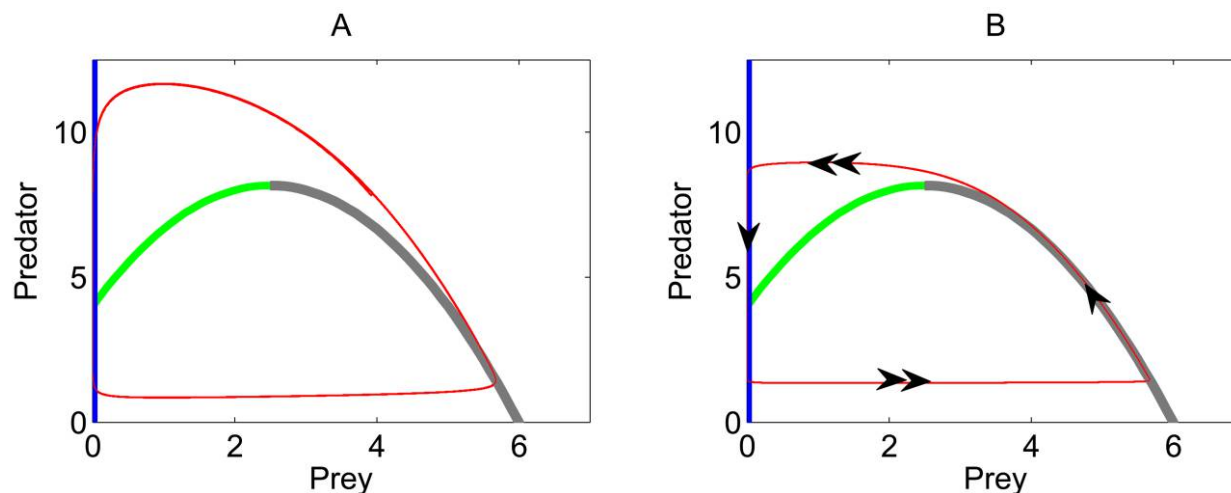


**Figure 2:** Example oscillatory dynamics (*red*) for the predator-prey system (1) with a fast-prey species. The predator (vertical) axis and the green and gray curves define the left, middle, and right branches of the critical manifold, respectively. Double arrows in *B* indicate the direction of fast flow, and the single arrows indicate the direction of the slow flow along the critical manifold.  $\epsilon = 1$  in *A* and  $0.1$  in *B*. Other parameters are  $a = 1$ ,  $b = 1$ ,  $d = 0.5$ ,  $h = 1$ ,  $K = 1.5$ , and  $r = 4$ .

We divide  $C$  into three different curves: a left ( $C_L$ ), a middle ( $C_M$ ), and a right ( $C_R$ ) branch. In figure 2*B*,  $C_L$  is the predator axis (*blue*) and together  $C_M$  (*green curve*) and  $C_R$  (*gray curve*) make up the prey nullcline. When solutions to system (1) are near the critical manifold, they behave as if they were on it. Thus, to understand how solutions of a fast-slow system behave, we need to understand what solutions on the critical manifold do, where they jump away from it, and where they land near it.

The single arrows in figure 2*B* indicate how trajectories move on or near the critical manifold. When near  $C_L$ , solutions move down, and when near  $C_R$ , solutions move up. Note that even though  $C$  is defined to be the equilibria of the fast variable, solutions will still move near  $C$  because the fast and slow variables are coupled. The double arrows in figure 2*B* indicate the stability of different parts of the branches. This stability dictates where solutions jump off of  $C$  (repelling behavior) and where they land on it (attracting behavior). In figure 2*B*, the lower set of double arrows indicates that the piece of  $C_L$  below the green curve is repelling and that  $C_R$  is attracting. The upper set of double arrows indicates that the apex of  $C_R$  is repelling and the part of  $C_L$  above the green curve is attracting.

Solutions of a fast-slow system behave in the following manner. First, a solution quickly runs near an attracting branch of the critical manifold. The solution then slowly moves as if constrained to that branch. If the solution encounters a stable equilibrium point on the branch, then the solution will go to that equilibrium. If it does not encounter one, then the solution will continue until it

reaches a jumping point. After jumping, the solution will quickly run to a second stable branch of the critical manifold, land, and repeat the sequence.

As an example, consider the trajectory in figure 2*B* and note that the equilibrium point for these parameter values is unstable and located on  $C_M$ . A solution starting near the lower set of double arrows quickly runs to  $C_R$ . Then the solution slowly moves up  $C_R$  until it nears the apex of the prey nullcline (where the  $C_M$  and  $C_R$  meet). Near the apex, the solution jumps off  $C_R$  and quickly runs to the upper part of  $C_L$ . Once near  $C_L$ , the solution moves down the predator axis until it jumps off somewhere below the intersection of  $C_L$  and  $C_M$  (where the green and blue curves intersect). The cycle then repeats.

There are two significant advantages to restricting our attention to the dynamics on the critical manifold instead of analyzing the full system. First, since the critical manifold is of lower dimension than the full system, the restriction makes the mathematical analysis simpler. For system (1), we can understand a two-dimensional model by analyzing one-dimensional branches of the critical manifold. Second, the dynamics that occur when  $\epsilon \approx 0$  can be used to understand and predict dynamics when  $\epsilon \approx 1$ . Consider the trajectory in figure 2*A* that spends almost no time near  $C_R$  when  $\epsilon = 1$  and the trajectory in figure 2*B* that spends almost half of its time near  $C_R$  when  $\epsilon = 0.1$ . As  $\epsilon$  decreases to 0, the position of  $C$  does not change and solutions stick closer to  $C$  for longer periods of time. In addition, the periodic orbit retains its qualitative shape as  $\epsilon$  becomes smaller. Thus, while we do not

necessarily believe that the prey species dynamics will be infinitely faster than those of the predator ( $\epsilon \approx 0$ ), that limit yields insight into the dynamics that occur when prey is moderately faster than the predator ( $\epsilon \approx 1$ ).

### Predator-Prey Model with Predator Evolution

Here we present a general predator-prey model with predator evolution that will be the focus of the article. Due to our model's level of generality, a system with predator evolution can be transformed into a system with prey evolution mathematically by reversing time (see app. A). Most results carry over between the two cases (see app. F). Differences that arise between the two types of evolution will be presented in "Predator-Prey Model with Prey Evolution."

Our general model for a predator-prey system ( $y$ ,  $x$ , respectively) with fast evolution of the mean predator trait value,  $\beta$ , is given by

$$\begin{aligned}\frac{dx}{dt} &= F(x) - G(x, y, \beta), \\ \frac{dy}{dt} &= H(x, y, \beta) - D(y, \beta), \\ \epsilon \frac{d\beta}{dt} &= B(\beta)V \frac{\partial}{\partial \beta} \left( \frac{1}{y} \frac{dy}{dt} \right).\end{aligned}\quad (3)$$

The  $F$  is the growth rate of the prey population in the absence of predation,  $G$  is the predation rate of the prey,  $H$  is the composition of the prey to predator conversion and predation rate of the prey, and  $D$  is the death rate of the predator population. The product  $B(\beta)V$  defines the additive genetic variance of the trait, where  $B(\beta)$  is a bounding function for the trait. A typical functional form we will use is  $B(\beta) = (\beta - \beta_{\min})(\beta_{\max} - \beta)$ , where  $\beta_{\min}$  and  $\beta_{\max}$  are the minimal and maximal values the trait can attain. Epsilon is a small positive value that flags the separation of timescales between the ecological and evolutionary processes. By decreasing the value of  $\epsilon$ , we speed up the rate of evolution (e.g., see fig. 1). Throughout the text, any variable subscripts denote partial derivatives; for example,  $H_\beta$  is short for  $\partial H / \partial \beta$ .

Typically the functions  $F$ ,  $G$ ,  $H$ , and  $D$  are written in terms of per capita growth rates,  $xf(x)$ ,  $xg(x, y, \beta)$ ,  $yh(x, y, \beta)$ , and  $yd(y, \beta)$ , respectively. We use the more general functions to simplify notation. Throughout the article we will assume the following about the functional responses in system (3). First,  $G$  and  $H$  are strictly increasing smooth functions of  $x$ ,  $y$ , and  $\beta$ . Second,  $D$  is a strictly increasing smooth function of  $y$  and  $\beta$ . Note that our assumptions about  $D$  and  $H$  being increasing functions of

$\beta$  implicitly define a trade-off for the trait, which in general will be density dependent. As the predator invests more in the trait and  $\beta$  increases, the predator birth rate will increase at the expense of a higher death rate.

The equation representing the trait dynamics in system (3) follows from the quantitative genetics approach derived in Lande (1982) and Abrams et al. (1993). The theory assumes that the mean trait value ( $\beta$ ) of a population changes at a rate proportional to both the additive genetic variance of the trait and the individual fitness gradient. This implies that the magnitude and direction of the selection pressure are determined by the fitness gradient of the trait,  $(\partial/\partial\beta)[(1/y)(dy/dt)]$ . Gradient dynamic approaches are a first approximation to many models, and their simplicity makes them analytically tractable (Abrams 2001, 2005). In addition, gradient dynamics models capture a range of behavior observed at the phenotypic level without having to specify gene-level processes. Thus, they are a good way to begin to understand the behavior of ecoevolutionary models but may yield an incomplete picture when specifics about the complexities of the genetic processes matter.

The direction and magnitude of the selection pressure can be both density and frequency dependent. When selection is frequency dependent, the trait equation in system (3) involves the gradient with respect to the fitness of the invader's phenotype instead of the resident's phenotype:

$$\epsilon \frac{d\beta}{dt} = B(\beta)V \frac{\partial}{\partial \beta} \left[ \frac{1}{y} (H(x, y, \beta, \hat{\beta}) - D(y, \beta, \hat{\beta})) \right] \bigg|_{\hat{\beta}=\beta}. \quad (4)$$

We will consider the special case where selection is frequency independent. Thus, fitness will not depend on the frequency of trait values, and an individual with a new trait  $\hat{\beta}$  will invade and replace a population with mean trait  $\beta$  if the relative fitness of the invading individual is higher than that of an individual with the mean trait value. We use this special case of the theory due to its analytic tractability and as a first approach to studying the effects of rapid evolution on ecological dynamics.

### Fast-Slow Dynamics in the Ecoevolutionary Model (3)

When  $\epsilon$  is a small positive value, the dynamics of system (3) can be understood by knowing how solutions move on the critical manifold, where solutions jump off of it, and where they land on it. For system (3), points on the critical manifold  $C$  satisfy  $d\beta/dt = 0$ , or equivalently,

$$C = \{(x, y, \beta) : B(\beta)(H_\beta(x, y, \beta) - D_\beta(y, \beta)) = 0, y > 0\}. \quad (5)$$

We divide  $C$  into left, middle, and right branches, respectively defined as

$$C_L = \{(x, y, \beta) : x > 0, y > 0, \beta = \beta_{\min}\}, \quad (6)$$

$$C_M = \{(x, y, \beta) : (H_\beta(x, y, \beta) - D_\beta(y, \beta)) = 0, y > 0, \beta \in (\beta_{\min}, \beta_{\max})\}, \quad (7)$$

$$C_R = \{(x, y, \beta) : x > 0, y > 0, \beta = \beta_{\max}\}. \quad (8)$$

Instead of being one-dimensional curves, as in figure 2, each branch now is a two-dimensional surface or plane in three-dimensional space (see fig. 3).

To understand when trajectories jump off of and onto the critical manifold, we classify points on  $C$  as attracting or repelling. For a point  $\rho$  on  $C_M$ , the value of  $H_{\beta\beta} - D_{\beta\beta}$  evaluated at that point,  $H_{\beta\beta}(\rho) - D_{\beta\beta}(\rho)$ , is the potentially nonzero eigenvalue for the fast dynamics. When the eigenvalue is negative, the point will be attracting and trajectories will land on it. When the eigenvalue is positive, the point will be repelling and trajectories will jump from it. Similarly,  $B_\beta(\rho)(H_\beta(\rho) - D_\beta(\rho))$  is the potentially nonzero eigenvalue for the fast dynamics for points on  $C_L$  and  $C_R$ . To summarize, for a point  $\rho$  on  $C$ :

$$C_M : H_{\beta\beta}(\rho) - D_{\beta\beta}(\rho) < 0 \quad \text{Stable} \quad (9)$$

$$H_{\beta\beta}(\rho) - D_{\beta\beta}(\rho) > 0 \quad \text{Unstable} \quad (10)$$

$$C_L, C_R : B_\beta(\rho)(H_\beta(\rho) - D_\beta(\rho)) < 0 \quad \text{Stable} \quad (11)$$

$$B_\beta(\rho)(H_\beta(\rho) - D_\beta(\rho)) > 0 \quad \text{Unstable} \quad (12)$$

In total, landing points satisfy equation (9) or equation (11) and jumping points satisfy equation (10) or equation (12).

Solutions to system (3) behave in the following manner. First a trajectory quickly approaches an attracting piece of the critical manifold. During this time, the population densities do not change substantially. Once near the attracting piece, the trajectory moves along the critical manifold as if it were stuck to that surface. If the trajectory never leaves the attracting part of the surface, then it will stay near that surface for all time and go to a stable equilibrium point or periodic orbit. If instead the trajectory enters the repelling part of the surface, then the trajectory will jump away from that part of the critical manifold and land on an attracting part of the critical manifold. The trajectory then repeats the sequence.

As an intuitive example of how solutions move in our system, consider a water droplet falling from the sky onto a slanted roof suspended above a sidewalk. The direction of fast movement in the system is up and down. The sidewalk and roof are branches of the critical manifold.

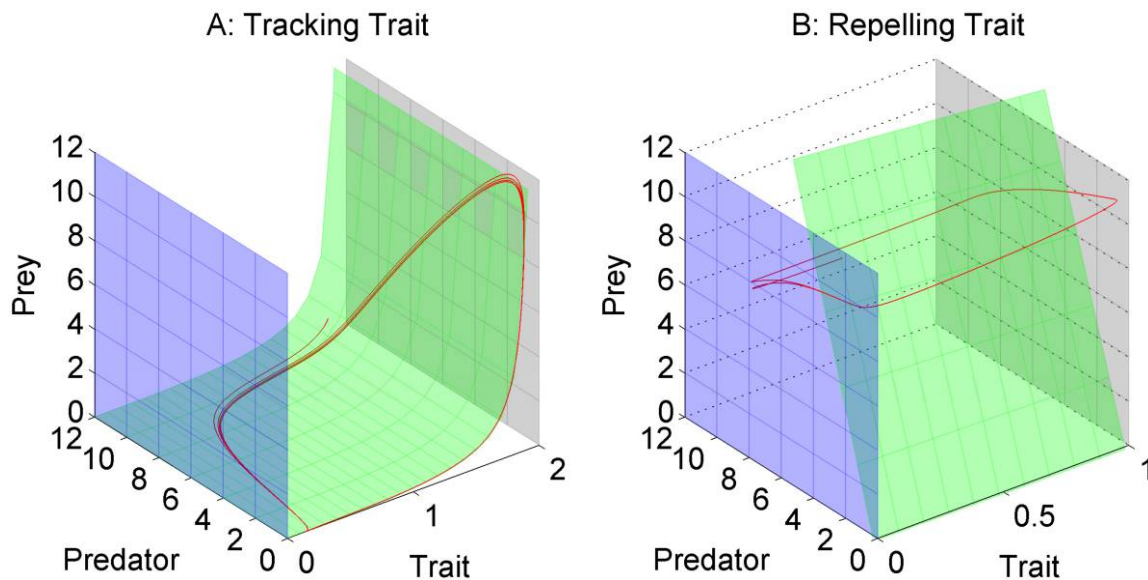


**Figure 3:** Example trajectories (red) for a predator-prey system with predator evolution where the trait is tracking (A) and repelling (B). The blue, green and gray planes define the left, middle, and right branches of the critical manifold, respectively. See appendix H for equations and parameter values.



Due to gravity, the droplet is attracted to the roof and very quickly falls onto it. Once on the slanted roof, the drop slowly moves toward the edge of the roof. This slow movement is just like the slow movement along the critical manifold. When the drop gets to the edge of the roof, again due to gravity, the droplet will be repelled from the roof edge and be attracted to the sidewalk. The water drop then quickly falls to the sidewalk and moves slowly along it. Trajectories in our system will essentially behave the same except that it will sometimes be possible for solutions to become trapped on the critical manifold at a stable equilibrium or periodic orbit. Going back to the water drop, this situation is analogous to the drop getting caught in a divot on the roof or sidewalk.

In figure 3 we present two examples of how trajectories can behave in our system. When selection favors intermediate trait values, all of  $C_M$  is attracting (eq. [9] always satisfied) and the trajectory stays near  $C_M$  for all time. When selection favors extreme values, all of  $C_M$  is repelling (eq. [10] always satisfied) and the trajectory alternates between being near  $C_L$  and being near  $C_R$ . We will refer to first case as a tracking trait and the second as a repelling trait.

## Results

### Local Stability Analysis

To begin understanding the effects of fast evolution, we first analyze how incorporating evolution into a predator-prey system changes the stability of the ecological dynamics. To do this, we compare the stability of an equilibrium point of system (3) to the stability of the same equilibrium point when we freeze evolution by setting  $d\beta/dt = 0$  (see app. C for details). In this section, we will consider only tracking traits (which represent stabilizing selection) and pay particular attention to cases where stable evolutionary dynamics either destabilize population dynamics that would head toward a stable equilibrium in the absence of evolution or stabilize population dynamics that would cycle in the absence of evolution.

As seen in theorem 2 of appendix C, the effect evolution has on the stability of the population dynamics depends on the sign of  $H_{x\beta}$ . Since  $H_\beta - D_\beta$  represents the strength of selection on the trait,  $H_{x\beta} = H_{x\beta} - D_{x\beta}$  represents how the strength of selection and the reward for investing in the trait increases or decreases as prey density increases. When  $H_{x\beta} > 0$ , the trait becomes more rewarding and the strength of selection increases as prey density increases. In this case, stable evolutionary dynamics increase the region of stability of the population dynamics and the inclusion of evolution in a system with cyclic population dynamics could lead to an equilibrium state for the populations.

When  $H_{x\beta} < 0$ , the trait becomes less rewarding and the strength of selection decreases as prey density increases. In this case, stable evolutionary dynamics decrease the region of stability of the population dynamics and the inclusion of evolution in an ecological system at equilibrium could lead to population oscillations. This result is quite counterintuitive since the trait ( $d\beta/dt$  equation) and population subsystems (system [3] with  $d\beta/dt = 0$ ) would tend to stable equilibria when decoupled but now cycle when coupled. These two results emphasizes that it is not enough to understand the stability of the evolutionary and ecological processes separately in order to determine the stability of the ecoevolutionary system.

To illustrate the above ideas we examine two examples. First, consider a modified Rosenzweig-MacArthur model (Rosenzweig and MacArthur 1963) with  $F = x(r - kx)$ ,  $G = H = bxy/(1 + cx/\beta)$ , and  $D = y(a\beta^2 + d)$  for some positive parameters  $a, b, c, d, r$ , and  $k$ . Here, increasing the predator's trait decreases the predator's handling time parameter at the cost of increasing the per capita death rate of the predator. Since the trait becomes increasingly rewarding as prey density increases ( $H_{x\beta} > 0$ ), the addition of evolution to a cycling ecological model can cause the populations to head toward a stable equilibrium (fig. 4A, 4B). For the second example, consider another modified Rosenzweig-MacArthur model where  $F = x(r - kx)$ ,  $G = H = bxy\beta/(1 + x\beta)$ , and  $D = y(a\beta + d)$ . Here the searching efficiency of the predator increases at the cost of an increased death rate as the predator invests more in the trait. Since increased investment in the trait increases the number of prey captured and therefore the total handling time, as prey density increases, investing in the trait will become less rewarding ( $H_{x\beta} < 0$ ). As seen in figure 4C and 4D, this allows for the case where the population dynamics tend to equilibrium when the trait is frozen but with the addition of stable evolutionary dynamics, the populations cycle for all time.

### Trade-Off Curves

One special case of system (3) of particular interest is when the effect of the trait on the predator recruitment and death rate is density independent. Mathematically, this means that the functional forms of the terms in system (3) factor as

$$\begin{aligned} H(x, y, \beta) &= h(x, y)\eta(\beta), \\ D(y, \beta) &= d(y)\delta(\beta). \end{aligned} \quad (13)$$

This factorization allows us to write  $\delta$  as a function of  $\eta$  (see app. D), which defines a trade-off curve between the proportional increase of the predator recruitment and the

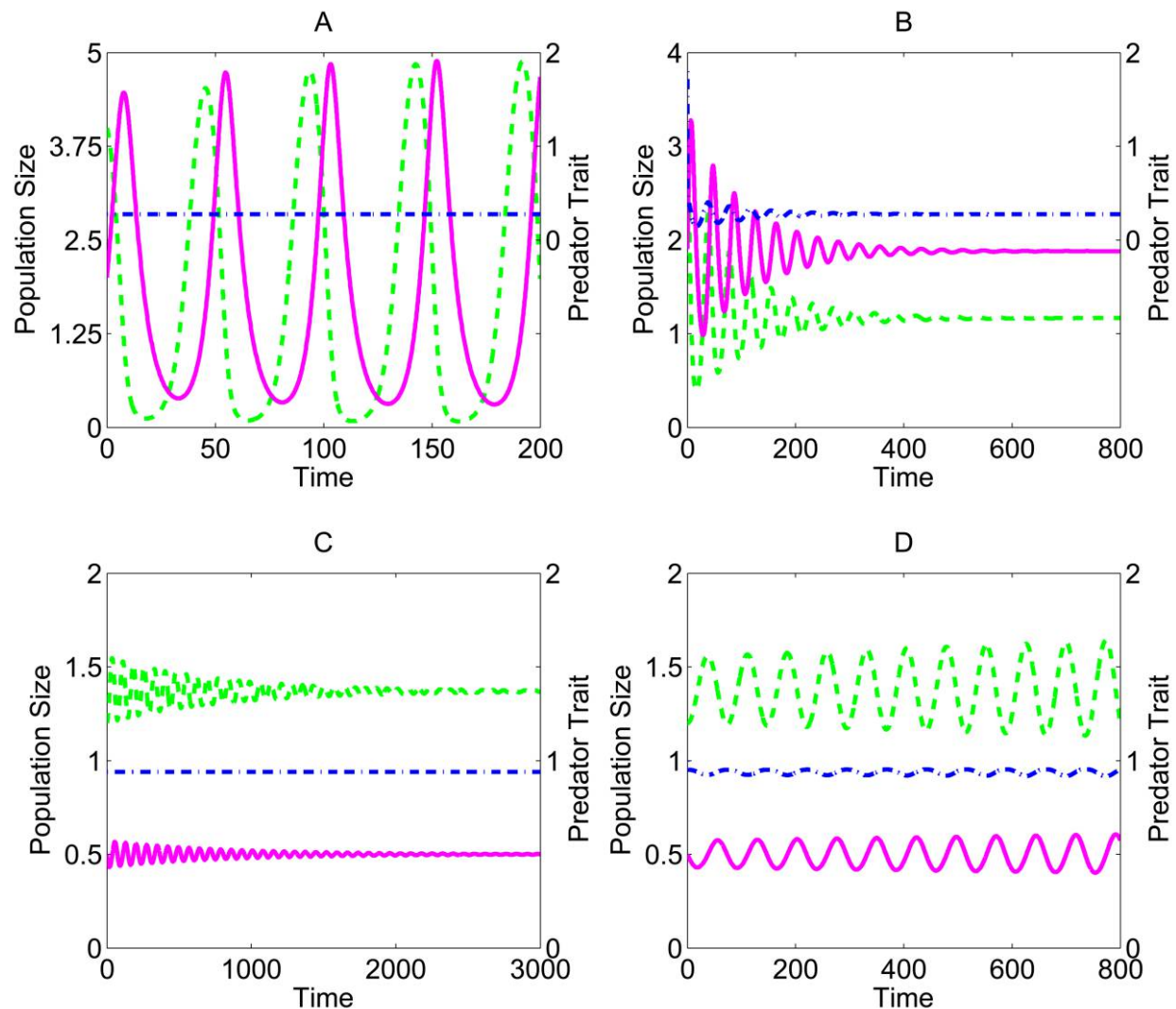


**Figure 4:** Two comparisons of predator (magenta), prey (green), and trait (blue) time series with predator evolution to their corresponding nonevolving system. In A, population dynamics cycle and trait dynamics tend to an equilibrium state when decoupled. When coupled, the population and trait dynamics tend to equilibrium (B). In C and D, population and trait dynamics tend to stable equilibria when decoupled, but when coupled the system is unstable and yields cyclic dynamics. In A and B,  $a = 3$ ,  $b = 1.86$ ,  $c = 0.1$ ,  $d = 1.3$ ,  $k = 0.4$ , and  $r = 2.95$ , and for the evolutionarily fixed dynamics  $\beta \approx 0.27$ . In C and D,  $b = 3.82$ ,  $c = 1$ ,  $d = 1.21$ ,  $k = 0.34$ , and  $r = 1.25$ , and for the evolutionarily fixed dynamics  $\beta \approx 0.94$ .

proportional increase of the predator death rate. Qualitative properties of the trade-off curve, defined by  $\delta(\eta)$ , can be used to predict qualitative properties of the population and trait time series, but the above factorization also limits the range of dynamical behavior a system can exhibit.

The concavity of the trade-off curve determines whether trait dynamics are stable or unstable (theorems 3 and 4 in app. D). For a trait value at  $\beta$ , if  $\delta(\eta)$  is concave up, then the trait dynamics are stable, and if  $\delta(\eta)$  is concave down, then the trait dynamics are unstable at  $\beta$ . This im-

plies that always concave-up trade-off curves yield tracking traits, and always concave-down trade-off curves yield repelling traits.

If the trade-off curve is always concave up, then the population dynamics either tend to equilibrium or exhibit predator-prey oscillations where the predator lags behind the prey with a phase lag of less than one-quarter of the cycle period. Examples of the second case are presented in figure 5A and 5C for two different trade-off curves. There are substantial quantitative differences between the oscillatory dynamics of figure 5A and 5C. The derivatives



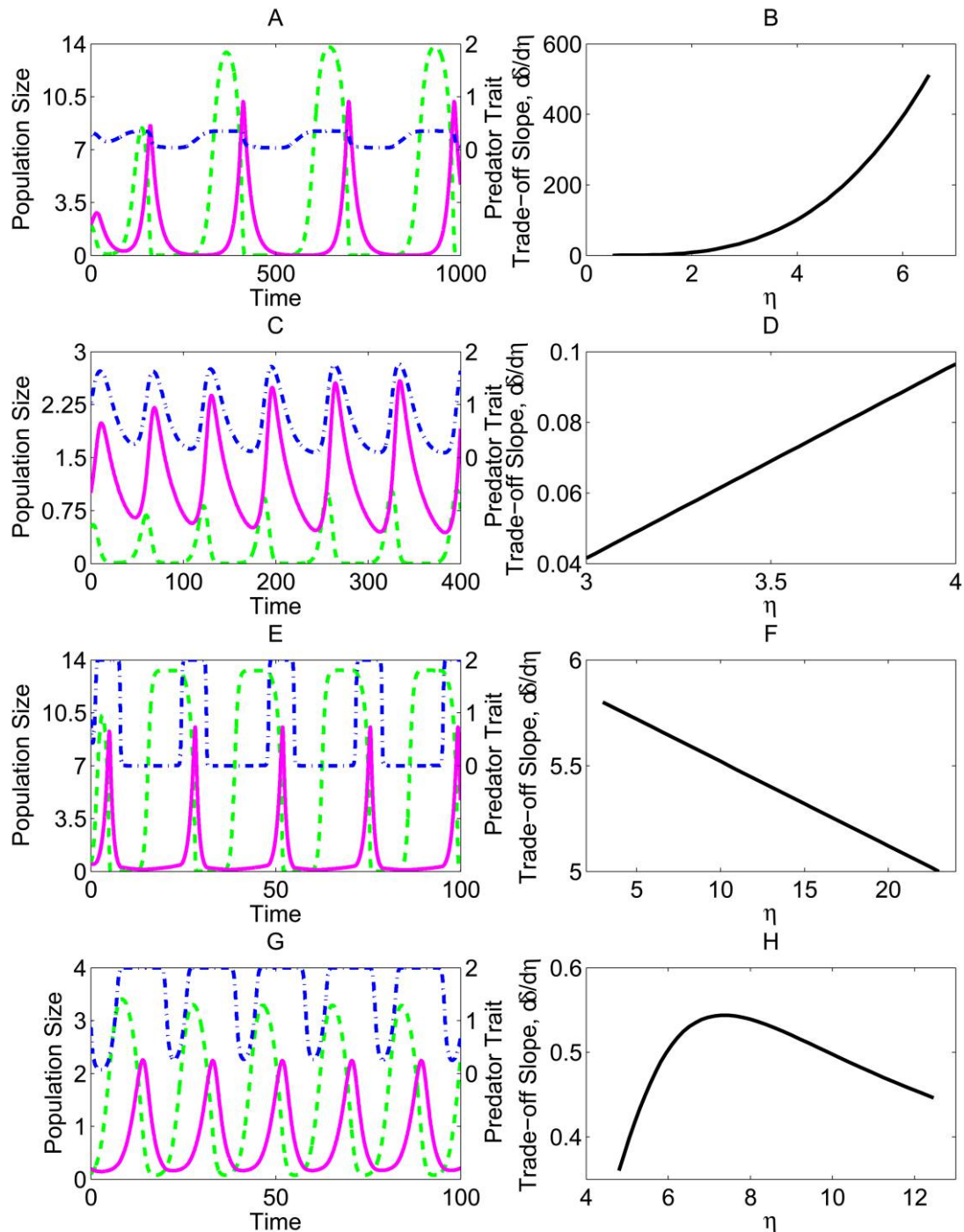


**Figure 5:** Examples of oscillating population and predator trait time series (*left*) with the derivative of the corresponding trade-off curve for the predator trait ( $d\delta/d\eta$ ; *right*) assuming the factorization in equation (13). Predator, prey, and trait dynamics are represented by the magenta, green, and blue curves, respectively. In A and B the trade-off curves are concave up, in C the curve is concave down, and in D the curve has a change in concavity. Situations where the population and trait dynamics go to equilibrium can occur for any concave-up trade-off curve. Equations and parameter values are given in appendix H.

of the trade-off curves allow one to distinguish between the different cases. In figure 5B, the derivative of the trade-off curve is large in magnitude and increasing very rapidly. Consequently, the large population fluctuations in figure 5A result in only small changes in the trait. If the curve resembles a straight line, that is, has little curvature as in figure 5D, then as depicted in figure 5C, small population oscillations will yield large trait fluctuations. For the intermediate case where the derivative is small in magnitude but still increasing, substantially large population oscillations will lead to large trait oscillations.

If the trade-off curve is always concave down, either the trait value converges to one of the extreme values and evolution ceases or the trait oscillates between the two extreme values of the trait (fig. 5E). These oscillations are known as relaxation oscillations in the fast-slow dynamical systems literature. We have numerically investigated a large number of models, and our findings suggest that while possible, relaxation oscillations of the trait are not the typical behavior of systems with a concave-down trade-off curve, and they occur only for a few initial conditions in very small ranges of parameter space. Furthermore, our numerical investigations suggest that the relaxation oscillations in the trait will not alter the population dynamics in a way that distinguishes them from the population dynamics occurring on the  $\beta_{\min}$  or  $\beta_{\max}$  plane. Thus, when the trade-off curve is always concave down, we can assume that the ecological dynamics will behave as if the trait is frozen either at  $\beta_{\min}$  or  $\beta_{\max}$ .

Finally we consider the case when the trade-off curve does not have constant concavity and instead has a sigmoid shape (fig. 5H). Since the trade-off curve has concave-up and concave-down sections, all of the dynamics in figure 5 can be observed with this trade-off curve. In addition, time series for an S-shaped trade-off curve can be a concatenation of those seen with a concave-up or concave-down trade-off curve. For example, the trait dynamics near  $\beta_{\max}$  in figure 5G resemble the relaxation oscillations in figure 5E, and near  $\beta_{\min}$ , the trait dynamics resemble those seen in figure 5C. While rare when the trade-off curve is concave down, relaxation oscillations are much more common in systems where the trade-off curve does not have constant concavity. Thus, in general, factoring of the functional responses does not prevent relaxation oscillation type dynamics.

#### *Boundary Plane Projections*

In this section, we present a simple graphical technique that allows one to predict the types of behavior and phenomena that arise with a repelling trait (e.g., fig. 3B). This graphical method allows us to not only determine what dynamics a particular model can exhibit but also to dis-

tinguish between different biological mechanisms that yield new ecological behavior. Furthermore, our approach has the computational advantage that we capture all of the information about the dynamics exhibited in the three-dimensional system (3) with two two-dimensional plots. By using the partial information contained in these two-dimensional plots to predict the dynamics that will occur in the full three-dimensional system, we can greatly reduce the amount of analysis needed to determine what types of behavior a particular model can exhibit.

To illustrate the idea behind the method, consider the trajectory in figure 3B. Because the trait is repelling, the trajectory in figure 3B oscillates between being very close to  $C_L$  (blue plane) and being very close to  $C_R$  (gray plane). Notice that the population densities do not change significantly when the trajectory jumps from one plane to the other. This suggests that the changes in predator and prey densities are solely determined by the behavior on the  $C_L$  and  $C_R$  planes. By understanding how the population densities change on these two planes and where the trajectory switches between planes (representing where the direction of selection switches), we can understand the behavior of the trajectory in the full three-dimensional picture.

To construct our graphic we need four pieces of information: the dynamics on  $C_L$ , the dynamics on  $C_R$ , and the points where trajectories will be repelled (jump) from each plane. The dynamics on  $C_L$  and  $C_R$  are determined by fixing the trait at  $\beta_{\min}$  and  $\beta_{\max}$ , respectively, in system (3). Trajectories on  $C_L$  or  $C_R$  will tend to stable equilibria or periodic orbits in those planes. We will refer to these stable objects as boundary attractors. The repelling points on each plane are those that satisfy equation (12), and the attracting points are those that satisfy equation (11). In our system, the repelling and attracting parts of the planes will be separated by a line defined by the intersection of  $C_M$  with  $C_L$  and  $C_R$ . In figure 3B, the repelling part of  $C_L$  is above the intersection with  $C_M$  (large prey values, small predator values) and the attracting part is below that line (small prey values, large predator values). The plane  $C_R$  is divided in the opposite way. Note that the division of the planes into attracting and repelling parts based on their intersection with  $C_M$  is exactly like the division of the gray curve in figure 2 into an attracting and a repelling piece.

The above information gives us two  $x, y$  planes that each contain a collection of stable attractors and a line separating the plane into repelling and attracting parts. To make the graphic, we superimpose these two planes on each other and look at one  $x, y$  plane. Going back to figure 3B, in essence we have removed  $C_M$  (green plane) and pushed  $C_L$  and  $C_R$  together. This collapse of three-dimensional  $(x, y, \beta)$  space gives us one two-dimensional  $(x, y)$

plane that contains the stable attractors, the repelling regions, and the attracting regions of both  $C_L$  and  $C_R$ .

Trajectories of the full system behave in the following way on the two-dimensional plot (see fig. 6B). The trajectory starts in the attracting region of  $C_L$  or  $C_R$  and approaches a stable attractor of that plane. While approaching the attractor, it may enter the repelling region of that plane. If it does, then the trajectory switches to following the dynamics in the opposite plane. This causes the trajectory to approach the stable object in the second plane. If the trajectory enters the repelling region of the second plane, then it will switch to following the dynamics in the first plane. When this cycle repeats indefinitely, the resulting population dynamics are a periodic orbit where the trait is cycling as well. If a trajectory stays in the attracting region of a plane for all time, then evolution will cease and the population dynamics will behave as if restricted to that plane for all time.

In the following, we present how the types and positions of the stable attractors in our two-dimensional graphic allow us to completely determine the dynamics exhibited in the three-dimensional model. To facilitate understanding, we will assume  $C_L$  and  $C_R$  have one stable attractor each and, whenever possible, that the curves separating the planes into attracting and repelling regions are parallel to the  $Y$ -axis. The analysis is the same when these assumptions are relaxed. Finally, in figure 6, trajectories will spend some time in the repelling region of a plane and not jump immediately before switching their behavior (e.g., fig. 6B). This behavior is common, though not the rule, and we use it to emphasize how trajectories will behave.

**Equilibrium-Equilibrium Case.** We begin with the simplest case, where  $C_L$  and  $C_R$  only have one stable equilibrium point. If at least one of the equilibria is located in the attracting region of its respective plane, then trajectories will converge to that equilibrium and evolution will cease. Cases where both equilibria are in the attracting region of their planes yield systems with bistability (fig. 6A). Since only one equilibrium needs to be in the attracting region of its plane to have evolution cease, an initial check for evolutionary convergence of a repelling trait is whether any equilibria are in the attracting regions of their planes.

Now assume each boundary contains a single equilibrium contained in the repelling region of the plane. These equilibria are saddles that are attracting in the  $x$  and  $y$  directions but repelling in the  $\beta$  direction. In our graphic, trajectories from such systems will alternate between approaching the  $C_L$  and  $C_R$  equilibria (see figs. 6B–6D and 7B for examples). In the full three-dimensional picture, trajectories behave as follows. First, the trajectory quickly runs close to the attracting region of one of the boundary

planes. Then, the trajectory slowly moves toward the equilibrium point as if it was restricted to that plane. As the trajectory approaches the equilibrium point, it will cross into the repelling region of that plane. Eventually the trajectory is repelled to the second plane, where it will behave as if constrained to that plane. As the trajectory approaches the equilibrium in the second plane, it will cross into the repelling region, run away to the first boundary plane, and repeat the cycle. This yields periodic behavior such as in figure 7A and 7B.

Qualitative properties of the above periodic orbits are determined by the relative positions of the two equilibria in the  $x, y$  plane. When one equilibrium has a greater predator density and a greater prey density than the other, classical cycles with a predator lag less than or equal to one-quarter of the period are observed (figs. 6B, 7A, and 7B). If the predator densities of both equilibria are equal and the densities of the prey sufficiently different, then the prey will cycle substantially while the predator population will remain relatively constant (fig. 6C). This phenomenon has been named “cryptic dynamics” (Yoshida et al. 2007). Finally, when one equilibrium has a greater predator density and a smaller prey density than the other, predator-prey oscillations with a lag greater than one-quarter of the period result (figs. 6D, 7C, and 7D). Cryptic dynamics and oscillations with a lag greater than one-quarter of the period are not observed in nonevolving systems.

All of the equilibria in figure 6A–6C are coexistence equilibria (both species have a positive density). Another case of interest is when one of the equilibria is an extinction equilibrium (predator density is 0). In this case, one of boundary equilibria is on the  $X$ -axis and in the ecological dynamics on that plane, the predator always becomes extinct. When the extinction equilibrium is in the attracting part of the plane, evolution leads to Darwinian extinction (Webb 2003; Parvinen 2005). If the extinction equilibrium is in the repelling region, then predator-prey cycles with a lag greater than one-quarter of the period are possible. In this case, our graphic looks like figure 6D except that the  $\beta_{\min}$  plane equilibrium (*blue equilibrium*) is on the  $X$ -axis.

**Periodic Orbit Case.** Assume either  $C_L$  or  $C_R$  has an equilibrium point in the repelling part of its plane and that the other has a periodic orbit partially in the repelling part of its plane. As in the previous case, the equilibrium and periodic orbit are stable in the  $x$  and  $y$  directions and (at least partially) repelling in the  $\beta$  direction. In our graphic, trajectories will alternate between approaching the equilibrium point and approaching and following the periodic orbit (fig. 6E–6G). In the full three-dimensional picture, trajectories behave as in the equilibrium-equilibrium case, except that now the trajectory will follow the path of the

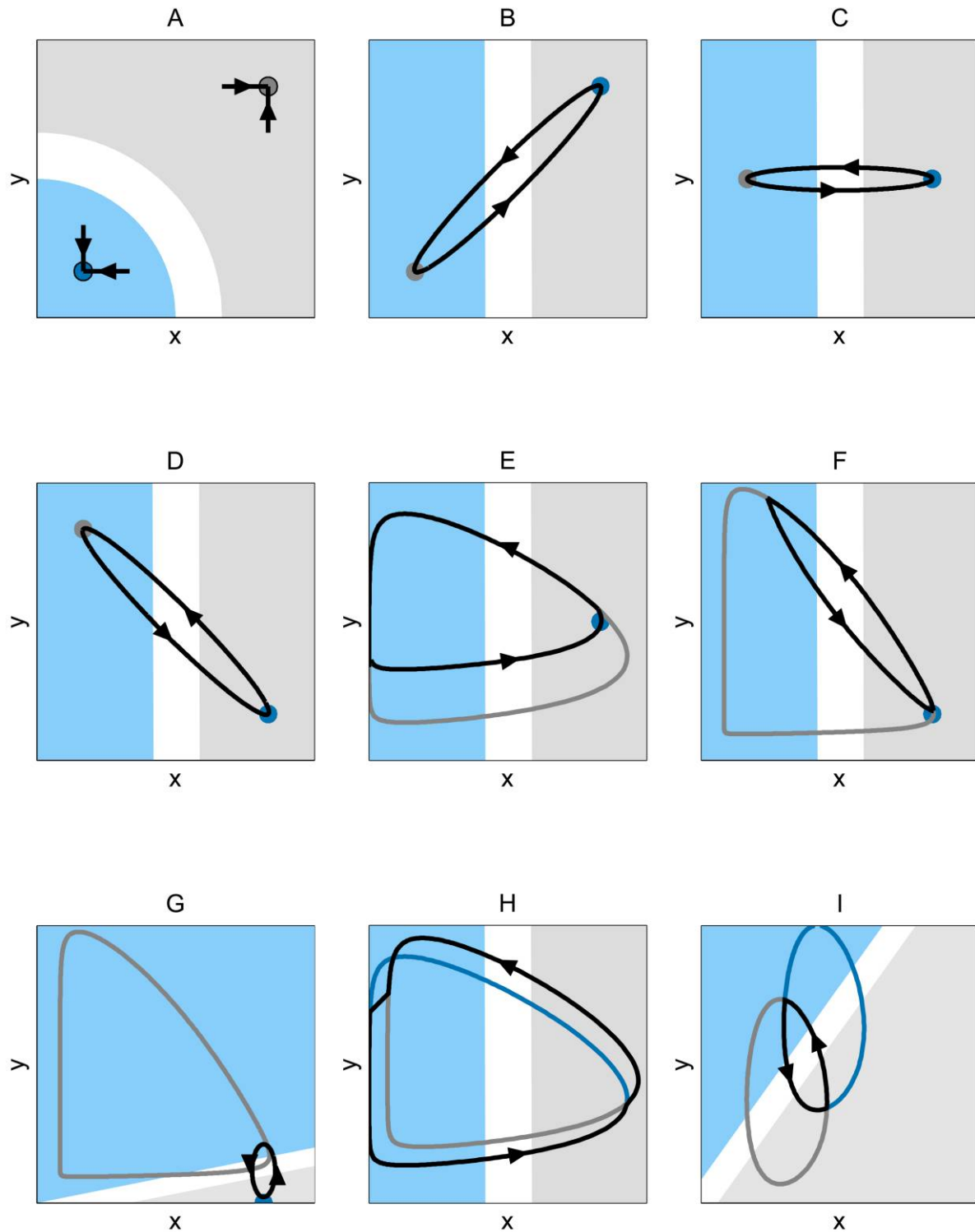


**Figure 6:** Qualitative representations of the dynamics that a predator-prey system with repelling predator trait dynamics can exhibit, projected onto the  $x, y$  plane. Dark blue (dark gray) equilibria or periodic orbits represent the stable limiting dynamics on the  $\beta_{\min}$  plane ( $\beta_{\max}$  plane). Black curves represent the observed population dynamics of the full evolving system projected onto the  $x, y$  plane. Light blue (light gray) regions correspond to population levels where the trait is decreasing (increasing) for all trait values. White regions correspond to population levels where the  $\beta_{\min}$  and  $\beta_{\max}$  planes are both locally attracting for the trait dynamics.

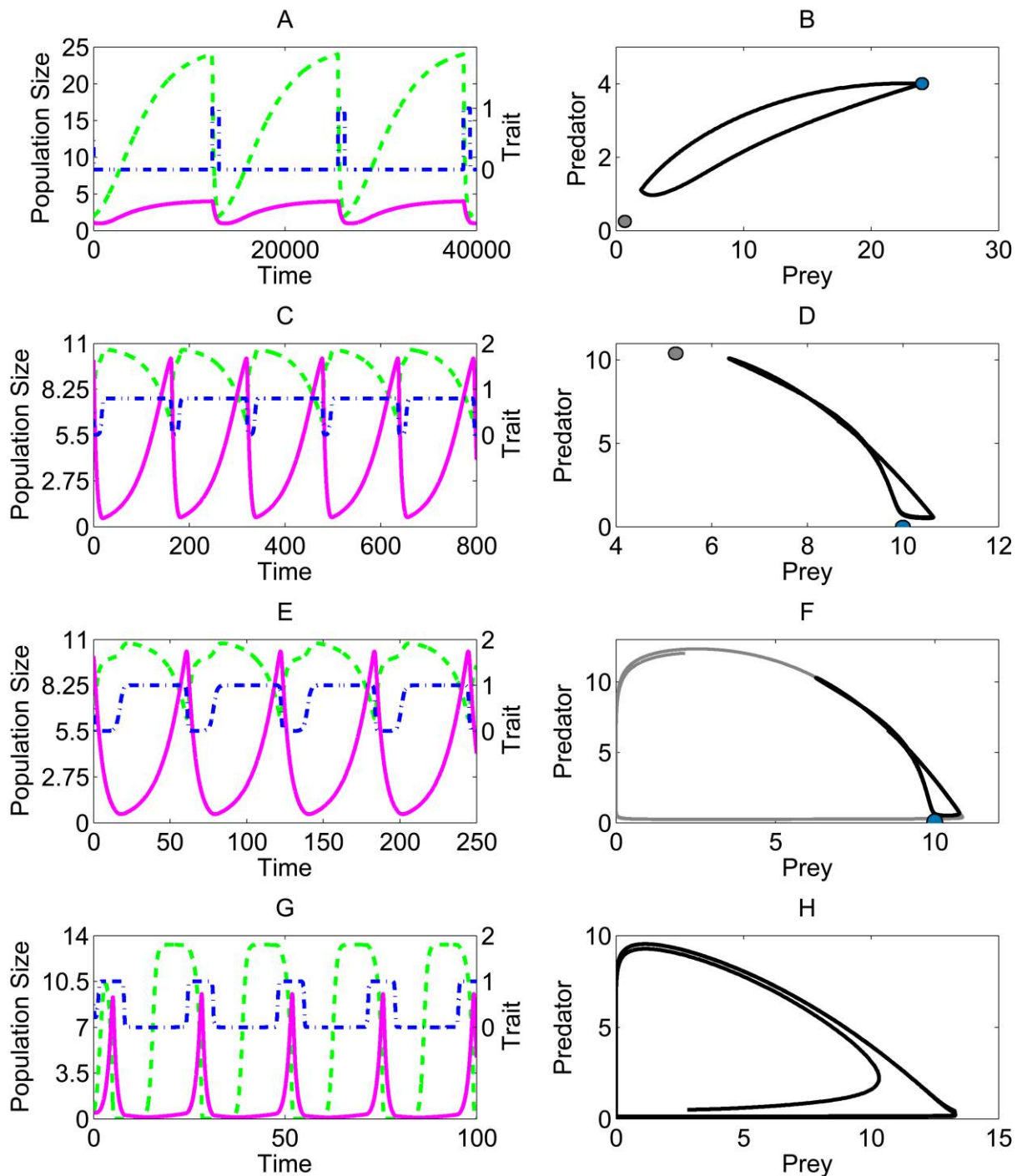


**Figure 7:** Examples of population and trait time series (left) for figure 6B (A), figure 8D (C), figure 8G (E), and figure 6H (G). A projection of the population dynamics onto the predator, prey plane (black curve) accompanies each example in the right column. For each projection a gray (blue) equilibrium or periodic orbit represents the stable attractor in the  $\alpha_{\min}$  or  $\beta_{\min}$  planes ( $\alpha_{\max}$  or  $\beta_{\max}$  planes). In H, the stable periodic orbits of the  $\beta_{\min}$  and  $\beta_{\max}$  planes lie almost exactly on top of the black orbit and are omitted.

periodic orbit into the repelling region before it jumps to the other plane. Note that the equilibrium can be an extinction equilibrium.

The positions of the equilibrium point, the periodic orbit, and the repelling regions of each boundary plane in the  $x, y$  plane affect the observed population oscillations. When a trajectory follows the boundary periodic orbit for a large proportion of its cycle (fig. 6E), the predator lags behind the prey with a lag less than one-quarter of the period. When a trajectory follows the boundary periodic orbit for a small proportion of its cycle, the lag becomes greater than one-quarter of the period and completely out-of-phase cycles are possible (figs. 6F and 7E). Cryptic dynamics can be observed when the equilibrium is below the right bend of the boundary periodic orbit and trajectories follow the periodic orbit for a brief amount of time (fig. 6G).

Finally, assume  $C_L$  and  $C_R$  both have a periodic orbit partially in their repelling regions. In our graphic, trajectories alternate between following each limit cycle for a portion of its orbit. This yields a periodic orbit that is a concatenation of the two periodic orbits (fig. 6H). The orientation of the two limit cycles determines whether the new periodic orbit will have a predator lag less than one-quarter of the period (figs. 6H and 7G) or a lag that is greater than one-quarter of the period (fig. 6I). Note that the orientation of the limit cycles presented in figure 6I is the only one through which out-of-phase oscillations can occur.

*When Do These Oscillatory Dynamics Occur?* Our graphic shows that three qualitatively different types of population oscillations can arise in predator-prey systems with predator evolution. While quarter-phase lag cycles (fig. 6E) are observed in the population dynamics of nonevolving systems, out-of-phase oscillations (fig. 6D, 6F) and cryptic dynamics (fig. 6C, 6G) cannot be seen unless evolution is present. Figure 7D and 7F depicts why this is the case. When out-of-phase cycles or cryptic dynamics occur in the three-dimensional system, the population dynamics projected onto the two-dimensional plane run along a single curve in both directions. Such behavior cannot occur in a two-dimensional system where such behavior would violate the uniqueness property of solutions to a system of two ordinary differential equations.

Even when evolution is present, most systems with a repelling trait cannot exhibit all three types of behavior. First, in order to have both of the boundary attractors partially in the repelling regions of their respective planes, we need  $H_{x\beta} > 0$  (see app. E). This means that as prey density increases, the trait must become increasingly rewarding and the strength of selection for larger trait values,  $H_\beta - D_\beta$ , must increase. If  $H_{x\beta} < 0$ , then the trait will al-

ways converge to either  $\beta_{\min}$  or  $\beta_{\max}$ . A second condition for trait oscillations is that if the predator functional responses  $H$  and  $D$  factor as in equation (13), then they must define an S-shaped trade-off curve (see "Trade-Off Curves").

As shown in appendix E, the dynamics in figure 6B–6D require additional constraints. First, the predator functional responses cannot factor as in equation (13). Second, the oscillations in those cases can be seen only when  $H$  is not an everywhere-increasing function of  $x$ . This implies that any standard functional response such as type I, II, or III will not be sufficient to see such dynamics. Instead, the prey must interfere with the predator's ability to capture prey when the prey are at high densities (e.g., a type IV functional response).

Finally, in general, when one boundary has an extinction equilibrium or a periodic orbit and the other has a coexistence equilibrium, there are fewer mathematical constraints on when these oscillations will arise (as compared to when both planes have only coexistence equilibria or periodic orbits). This trend suggests that the oscillations seen in this section are found most often when the  $\beta_{\min}$  and  $\beta_{\max}$  planes are on the opposite sides of a bifurcation that depends on the value of  $\beta$ . For example, in figure 6E the  $\beta_{\min}$  plane contains an attracting periodic orbit and the  $\beta_{\max}$  plane contains an attracting equilibrium point. If we treat  $\beta$  as a parameter, then as  $\beta$  increases toward  $\beta_{\max}$ , the population cycles that were present when  $\beta = \beta_{\min}$  disappear to give rise to an equilibrium state. We expect that bifurcations in the ecological dynamics depending on the trait value are the main mechanisms through which rapid trait evolution gives rise to dynamics that cannot occur in the absence of evolution.

#### *Predator-Prey Model with Prey Evolution*

The effects of predator and prey evolution are nearly equivalent. In this section, we present the differences that arise when the prey is the evolving species. This analysis shows that sometimes only ecological data and information are needed to determine which species is evolving in a predator-prey system. In the following,  $\alpha$  is the mean prey trait, where smaller values of  $\alpha$  protect the prey more (e.g., make it less edible) but come at a large cost. The prey-evolution model and all results about it that agree with the predator-evolution model are contained in appendix F.

*Prey Boundary Plane Projections.* Using the method in "Boundary Plane Projections," a superposition of the dynamics on the  $\alpha_{\min}$  and  $\alpha_{\max}$  boundary planes can be constructed. All of the dynamics presented in figure 6 with predator evolution are possible in figure 8 with prey evo-



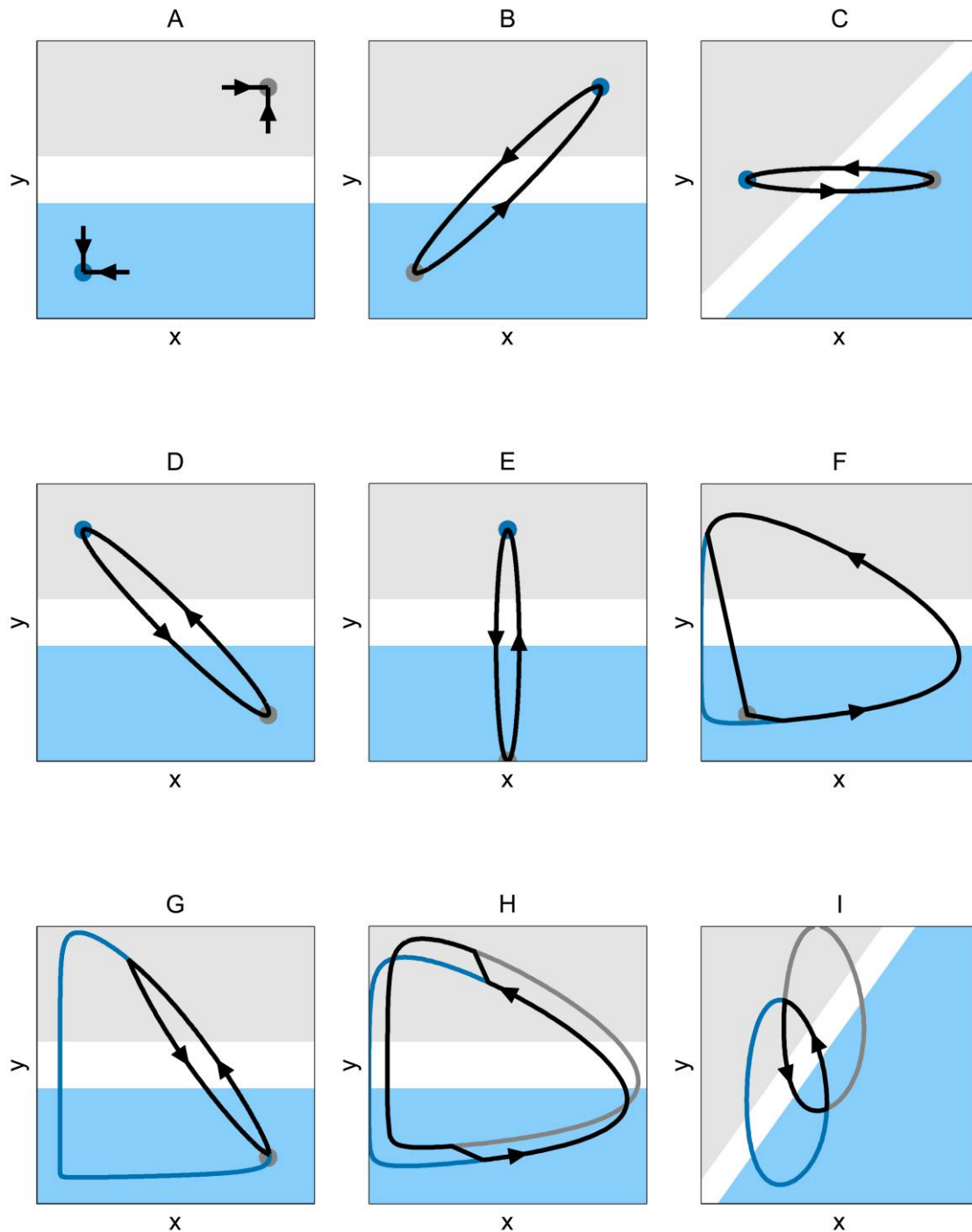


**Figure 8:** Qualitative representations of the dynamics that a predator-prey system with unstable prey trait dynamics can exhibit, projected onto the  $x, y$  plane. Dark blue (dark gray) equilibria or periodic orbits represent the stable limiting dynamics on the  $\alpha_{\max}$  plane ( $\alpha_{\min}$  plane). Black curves represent the observed population dynamics of the full evolving system projected onto the  $x, y$  plane. Light blue (light gray) regions of the  $x, y$  plane correspond to population levels where the trait is increasing (decreasing) for all trait values. White regions correspond to population levels where the  $\beta_{\min}$  and  $\beta_{\max}$  planes are both locally attracting for the trait dynamics. The association of colors with figure 6 is that blue signifies the direction of selection being better for the nonevolving species and gray being worse for the nonevolving species.

lution. Additional types of dynamical behavior are also possible when the prey is the evolving species. When the  $\alpha_{\min}$  equilibrium is an extinction equilibrium, that is, when freezing the prey trait at  $\alpha_{\min}$  would lead to predator extinction, dynamics such as those in figure 8B and 8E are possible. These two cases are not possible with predator evolution when an extinction equilibrium is present.

Prey evolution also generates dynamics such as those in figure 8C and 8D with fewer biological assumptions than the predator evolution case. With predator evolution, predation interference caused by the prey (e.g., type IV functional response) was necessary to get figure 6C and 6D. With prey evolution, such dynamics arise naturally and without extra assumptions about the system. This observation is of use to experimentalists working with predator-prey systems where it is unclear which species is evolving. If such interference is known to be absent from a system, then out-of-phase population cycling or cryptic dynamics lends evidence toward the prey being the evolving species.

*Phase Relations with Tracking Traits.* Ecological oscillations where the predator lags behind the prey with a lag that is less than one-quarter of the period are typical of an evolutionarily fixed system (Bulmer 1975). Predator-prey cycles where the lag is greater than one-quarter of the period, as in figure 1, suggest that evolution is occurring in the system. Such oscillations are easily generated with a repelling trait (see “Boundary Plane Projections”). Following Bulmer (1975), we investigate when such oscillations can arise with a tracking trait.

As shown in appendix G, a tracking predator trait cannot change the lag, and in such cases the ecological processes dictate the lag in the population dynamics. The same is not true for prey evolution. When the prey trait is tracking, the lag between the predator and prey oscillations depends on the quantity (see app. G)

$$Q = H_y - D_y + \frac{H_\alpha G_{y\alpha}}{F_{\alpha\alpha} - G_{\alpha\alpha}}. \quad (14)$$

The sign of  $Q$  determines whether the lag is greater or less than one-quarter of the period of the oscillations. When  $Q$  is negative, the lag is less than one-quarter of the period and tends to 0 as  $Q$  tends to negative infinity. When  $Q$  is positive, the lag is greater than one-quarter of the period and tends to half of the period as  $Q$  tends to positive infinity. When evolution is absent,  $Q = H_y - D_y$ . Thus, the sign of  $H_\alpha G_{y\alpha}/(F_{\alpha\alpha} - G_{\alpha\alpha})$  determines how the lag changes with the addition of prey evolution. Since we expect  $H_y - D_y \leq 0$  (Bulmer 1975) and assume  $F_{\alpha\alpha} - G_{\alpha\alpha} < 0$  and  $H_\alpha > 0$ , the change in the lag due to evolution is determined by the sign of  $G_{y\alpha}$ .

The quantity  $G_{y\alpha} = -(\partial/\partial y)(F_\alpha - G_\alpha)$  describes how the

strength of selection increases or decreases as the number of predators increases. When the trait becomes increasingly rewarding as predator density increases,  $G_{y\alpha} > 0$ , and prey evolution decreases the phase delay between the predator and prey oscillations. When the trait becomes less rewarding as predator density increases,  $G_{y\alpha} < 0$ , and prey evolution increases the phase delay between predator and prey oscillations. In particular, if  $G_{y\alpha} < 0$  and  $H_\alpha G_{y\alpha}/(F_{\alpha\alpha} - G_{\alpha\alpha})$  is large enough, then the phase difference between the oscillations will be greater than one-quarter of the period.

We propose two biological mechanisms through which the magnitude of  $H_\alpha G_{y\alpha}/(F_{\alpha\alpha} - G_{\alpha\alpha})$  will be large enough. First, assume that a small investment in the prey trait causes a large decrease in the predator's ability to consume and convert prey. Mathematically, this would imply that  $H_\alpha$  is very large. In the second mechanism, assume the trade-off in the trait is nearly linear. This results in lack of curvature in the fitness gradient and  $F_{\alpha\alpha} - G_{\alpha\alpha}$  being very small.

The above results in combination with those from “Prey Boundary Plane Projections” imply that population oscillations with a lag greater than one-quarter period will most likely be the result of prey evolution. Thus, if such oscillations are observed and an experimentalist is deciding on which species to investigate more closely for signs of rapid evolution, without extra information, the prey species is the better starting point. In addition, if tracking prey evolution is determined to be the cause of the oscillations, then the driving mechanism can be determined by measuring the effect evolution has on predator consumption ( $H_\alpha$ ) and the curvature of the trade-off curve ( $F_{\alpha\alpha} - G_{\alpha\alpha}$ ).

## Discussion

Throughout the past 2 decades theoreticians have studied particular models and systems to understand the effects of rapid evolution on population dynamics in predator-prey systems. To gain insight into how new phenomena arise in such systems due to rapid evolution, we examined the extreme case where evolutionary processes are much faster than their ecological counterparts. In using this approach, we are not positing that evolution occurs at instantaneous rates. Rather, the information obtained by studying the fast limit illuminates ecoevolutionary dynamics that occur when evolutionary and ecological process have comparable timescales.

The main benefit from the analytical tractability and generality gained by working in the fast-evolution limit is a better understanding of the links between individual-level mechanisms and population-level phenomena in ecoevolutionary dynamics. Our approach shows that qual-

itative properties of a trade-off curve predict how population dynamics affect oscillations in the trait and the range of phenotypes observed (fig. 5). In addition, since trade-off curves lead to a particular factorization of predator functional responses, the shape of the trade-off curve can determine the range of ecological and evolutionary dynamics that can occur.

Explicit assumptions about the predator and prey functional responses also play an important role in determining the range of behavior systems can exhibit. With prey evolution, assumptions about the trait's effect on predator recruitment and the curvature of its trade-off determine whether out-of-phase oscillations can arise from a tracking trait. For predator evolution, more complex interactions between the predator and prey species (e.g., type IV functional response) are necessary to realize specific mechanisms through which new behaviors, such as cryptic dynamics, arise. With either species evolving, oscillatory dynamics of the trait, completely out-of-phase oscillations, and the destabilization of ecological dynamics by a stable trait are possible only in systems with predator satiation and a complex density-dependent trade-off for the trait.

Finally, by comparing the effects of predator and prey evolution, we observed that predator-prey oscillations where the predator lags behind the prey by more than one-quarter of the period are much more common in systems where the prey is the evolving species. In some cases, extra ecological information about the system, such as the absence of a type IV functional response, will suffice to infer that prey evolution is occurring. Thus, we can make predictions about evolutionary processes from purely ecological data.

Some of the above conclusions also act as cautionary notes for experimentalists and modelers. First, while rapid evolution in a predator-prey system can allow for population dynamics that are not possible in evolutionarily fixed systems, one must be careful about assumptions that prevent these dynamics from occurring. Because of their simplicity, functional responses that factor as in equation (13) have been used in the literature to investigate the effects of evolution (e.g., Khibnik and Kondrashov 1997; Law et al. 1997). Biologically, this implies that a trade-off curve exists and that the effects of the trait are independent of the densities of the predator and prey species. In this case, the oscillations in figures 6–8 and the destabilization of ecological dynamics by a stable trait in figure 4C and 4D are not possible. Thus, simplifying biological assumptions used in data collection and model selection can lead to an incomplete understanding of a system and leave new or unique behavior unexplained.

A second cautionary note is sounded by figure 4C and 4D, where the stability of the ecoevolutionary dynamics cannot be predicted from the behavior of the decoupled

evolutionary and ecological processes. It is very generally true that the dynamics of interspecific population interactions and coevolution cannot be predicted by understanding each component separately. The phenomenon in figure 4 has been observed for specific cases of our model. Abrams (1992) examined a particular family of functional forms for the predator recruitment term  $H$  and found that destabilization of population dynamics with a stable trait required sufficiently rapid evolution and a nonlinear dependence of  $H$  on the predator trait. Our generalization of the second condition is  $H_{x\beta} < 0$  from “Local Stability Analysis.” Abrams and Matsuda (1997b) also noted that predator satiation was necessary to destabilize population dynamics, though their results are not directly comparable since their system does not satisfy equations (9) or (10).

When new phenomena do arise, our analysis offers analytical conditions and graphical methods that allow one to identify mechanisms driving the ecological dynamics in an evolving system. Given time series data for a system where selection favors extreme phenotypes, the graphics in figures 6 and 8 allow one to identify the potential mechanisms that are driving the dynamics. With further ecological information about the dynamics exhibited by the extreme phenotypes (e.g., equilibrium-equilibrium case) or ecological processes (e.g., absence of a type IV functional response), the correct mechanism and the evolving species can be deduced.

This graphic can also be applied to predator-prey systems where selection is frequency dependent. Two of the mechanisms presented in “Prey Boundary Plane Projections” have been observed experimentally where frequency-dependent selection was present. Out-of-phase cycles were generated from the scenario in figure 8G of Yoshida et al. (2003), and cryptic dynamics generated by the scenario in figure 6G (but where the prey is evolving) were observed by Bohannan and Lenski (2000). Thus, our projection method can yield information about the dynamics possible in systems with frequency-dependent and independent selection, but it is unclear whether any new dynamics can arise with frequency dependent selection.

Studies by Bohannan and Lenski (2000) and Yoshida et al. (2003) also demonstrate how the analysis at the fast-evolution limit can yield insight for biological systems where ecological and evolutionary changes are occurring at the same rate. In both systems, evolution was not occurring faster than the population dynamics, yet the theory still accurately predicted the dynamics. In this study, we have emphasized this point numerically by presenting only numerical simulations where  $\epsilon \geq 0.1$ —a value considered large for fast-slow systems theory.

The previous two points suggest that similar analyses could be useful in other areas where ecoevolutionary dynamics are important. One area where ecological and evo-

lutionary processes can have comparable timescales is host-pathogen systems (Earn et al. 2002; Grenfell et al. 2004). Recent studies have begun to emphasize the need to understand the interplay between these processes when considering vaccination strategies and the evolution of drug resistance and virulence (Grenfell et al. 2004; Gandon and Day 2007). Studying the fast evolution limit could yield insight into the complicated behavior observed in these systems.

Finally, we consider the advantages and disadvantages of applying the theory presented in this study to predator-prey and other exploiter-victim systems. Since gradient dynamics approaches are a first approximation to many models, they capture a range of behavior observed at the phenotypic level without having to specify specific gene level processes (Abrams 2001, 2005). In addition, gradient dynamic approaches allow one to study how ecological and evolutionary processes influence each other at any separation of timescales. Their simplicity and versatility makes them a good way to begin to understand the types of behavior exhibited by ecoevolutionary models. The disadvantage of this approach arises when specifics about the genetic processes matter and assumptions in the theory break down (e.g., near evolutionary branching points and when invasion does not guarantee persistence). Because of their simplifying assumptions, gradient dynamic approaches cannot account for these complexities and more detailed models are needed.

This study exemplifies how fast-slow dynamical systems theory offers a clear viewpoint through which the effects of evolution on ecological dynamics can be studied. The reduction in dimension and the resulting analytical tractability of this methodology makes it a powerful tool for understanding the interplay between ecological and evolutionary processes. Furthermore, while the theory requires a large separation of timescales, it still offers understanding about cases where that assumption is relaxed. Thus, we think the approach followed in this study is a step forward toward developing a general theory for eco-evolutionary dynamics.

### Acknowledgments

We thank B. Dalziel, M. Holden, P. Hurtado, C. Kuehn, K. Marchetto, J. Wynne, and two anonymous reviewers for suggestions and helpful comments on an earlier version of this manuscript. This research was supported by a James S. McDonnell Foundation research award, the National Science Foundation (DEB-0813743), and an Alfred P. Sloan Foundation graduate fellowship to M.H.C.

### Literature Cited

- Abrams, P. A. 1992. Adaptive foraging by predators as a cause of predator-prey cycles. *Evolutionary Ecology* 6:56–72.
- . 2001. Modelling the adaptive dynamics of traits involved in inter- and intraspecific interactions: an assessment of three models. *Ecology Letters* 4:166–175.
- . 2005. “Adaptive Dynamics” vs. “adaptive dynamics.” *Journal of Evolutionary Biology* 18:1162–1165.
- Abrams, P. A., and H. Matsuda. 1997a. Fitness minimization and dynamic instability as a consequence of predator-prey coevolution. *Evolutionary Ecology* 11:1–20.
- . 1997b. Prey adaptation as a cause of predator-prey cycles. *Evolution* 51:1742–1750.
- Abrams, P. A., H. Matsuda, and Y. Harada. 1993. Evolutionarily unstable fitness maxima and stable fitness minima of continuous traits. *Evolutionary Ecology* 7:465–487.
- Arnold, L., C. K. R. T. Jones, K. Mischaikow, and G. Raugel. 1995. Geometric singular perturbation theory. Pages 44–188 in R. Johnson, ed. *Dynamical systems*. Vol. 1609. *Lecture Notes in Mathematics*. Springer, Berlin.
- Bailey, J. K., J. A. Schweitzer, F. Ubeda, J. Koricheva, C. J. LeRoy, M. D. Madritch, B. J. Rehill, et al. 2009. From genes to ecosystems: a synthesis of the effects of plant genetic factors across levels of organization. *Philosophical Transactions of the Royal Society B: Biological Sciences* 364:1607–1616.
- Bohannan, B. J. M., and R. E. Lenski. 2000. Linking genetic change to community evolution: insights from studies of bacteria and bacteriophage. *Ecology Letters* 3:362–377.
- Bulmer, M. G. 1975. Phase relations in the ten-year cycle. *Journal of Animal Ecology* 44:609–621.
- Conover, D. O., and S. B. Munch. 2002. Sustaining fisheries yields over evolutionary time scales. *Science* 297:94–96.
- Dercole, F., R. Ferriere, A. Gagnani, and S. Rinaldi. 2006. Coevolution of slow-fast populations: evolutionary sliding, evolutionary pseudo-equilibria and complex Red Queen dynamics. *Proceedings of the Royal Society B: Biological Sciences* 273:983–990.
- Earn, D. J. D., J. Dushoff, and S. A. Levin. 2002. Ecology and evolution of the flu. *Trends in Ecology & Evolution* 17:334–340.
- Ezard, T. H. G., S. D. Cote, and F. Pelletier. 2009. Eco-evolutionary dynamics: disentangling phenotypic, environmental and population fluctuations. *Philosophical Transactions of the Royal Society B: Biological Sciences* 364:1491–1498.
- Fussmann, G. F., S. P. Ellner, K. W. Shertzer, and N. G. Hairston Jr. 2000. Crossing the Hopf bifurcation in a live predator-prey system. *Science* 290:1358–1360.
- Fussmann, G. F., M. Loreau, and P. A. Abrams. 2007. Eco-evolutionary dynamics of communities and ecosystems. *Functional Ecology* 21:465–477.
- Gandon, S., and T. Day. 2007. The evolutionary epidemiology of vaccination. *Journal of the Royal Society Interface* 4:803–817.
- Grant, P. R., and B. R. Grant. 2002. Unpredictable evolution in a 30-year study of Darwin’s finches. *Science* 296:707–711.
- Grenfell, B. T., O. G. Pybus, J. R. Gog, J. L. N. Wood, J. M. Daly, J. A. Mumford, and E. C. Holmes. 2004. Unifying the epidemiological and evolutionary dynamics of pathogens. *Science* 303:327–332.
- Hairston, N. G., Jr., and T. A. Dillon. 1990. Fluctuating selection and response in a population of freshwater copepods. *Evolution* 44:1796–1805.
- Hairston, N. G., Jr., and W. E. Walton. 1986. Rapid evolution of a life history trait. *Proceedings of the National Academy of Sciences of the USA* 83:4831–4833.
- Hairston, N. G., Jr., W. Lampert, C. E. Caceres, C. L. Holtmeier, L.

- J. Weider, U. Gaedke, J. M. Fischer, J. A. Fox, and D. M. Post. 1999. Rapid evolution revealed by dormant eggs. *Nature* 401:446.
- Hanski, I., and I. Saccheri. 2006. Molecular-level variation affects population growth in a butterfly metapopulation. *PLoS Biology* 4: 719–726.
- Heath, D. D., J. W. Heath, C. A. Bryden, R. M. Johnson, and C. W. Fox. 2003. Rapid evolution of egg size in captive salmon. *Science* 299:1738–1740.
- Johnson, M. T. J., M. Vellend, and J. R. Stinchcombe. 2009. Evolution in plant populations as a driver of ecological changes in arthropod communities. *Philosophical Transactions of the Royal Society B: Biological Sciences* 364:1593–1605.
- Jones, L. E., and S. P. Ellner. 2007. Effects of rapid prey evolution on predator-prey cycles. *Journal of Mathematical Biology* 55:541–573.
- Jones, L. E., L. Becks, S. P. Ellner, N. G. Hairston Jr., T. Yoshida, and G. F. Fussmann. 2009. Rapid contemporary evolution and clonal food web dynamics. *Philosophical Transactions of the Royal Society B: Biological Sciences* 364:1579–1591.
- Khibnik, A. I., and A. S. Kondrashov. 1997. Three mechanisms of Red Queen dynamics. *Philosophical Transactions of the Royal Society B: Biological Sciences* 264:1049–1056.
- Kinnison, M. T., and N. G. Hairston Jr. 2007. Eco-evolutionary conservation biology: contemporary evolution and dynamics of persistence. *Functional Ecology* 21:444–454.
- Kinnison, M. T., M. J. Unwin, and T. P. Quinn. 2008. Eco-evolutionary vs. habitat contributions to invasion in salmon: experimental evaluation in the wild. *Molecular Ecology* 17:405–414.
- Lande, R. 1982. A quantitative genetic theory of life history evolution. *Ecology* 63:607–615.
- Law, R., P. Marrow, and U. Dieckmann. 1997. On evolution under asymmetric competition. *Evolutionary Ecology* 11:485–501.
- Meyer, J. R., S. P. Ellner, N. G. Hairston Jr., L. E. Jones, and T. Yoshida. 2006. Prey evolution on the time scale of predator-prey dynamics revealed by allele-specific quantitative PCR. *Proceedings of the National Academy of Sciences of the USA* 103:10690–10695.
- Palkovacs, E. P., M. C. Marshall, B. A. Lamphere, B. R. Lynch, D. J. Weese, D. F. Fraser, D. N. Reznick, C. M. Pringle, and M. T. Kinnison. 2009. Experimental evaluation of evolution and coevolution as agents of ecosystem change in Trinidadian streams. *Philosophical Transactions of the Royal Society B: Biological Sciences* 364:1617–1628.
- Palumbi, S. R. 2001. Humans as the world's greatest evolutionary force. *Science* 293:1786–1790.
- Parvinen, K. 2005. Evolutionary suicide. *Acta Biotheoretica* 53:241–264.
- Pelletier, F., T. Clutton-Brock, J. Pemberton, S. Tuljapurkar, and T. Coulson. 2007. The evolutionary demography of ecological change: linking trait variation and population growth. *Science* 315:1571–1574.
- Post, D. M., and E. P. Palkovacs. 1997. Eco-evolutionary feedbacks in community and ecosystems ecology: interactions between the ecological theatre and the evolutionary play. *Philosophical Transactions of the Royal Society B: Biological Sciences* 364:1629–1640.
- Reznick, D. N., F. H. Shaw, F. H. Rodd, and R. G. Shaw. 1997. Evaluation of the rate of evolution in natural populations of guppies (*Poecilia reticulata*). *Science* 275:1934–1937.
- Reznick, D. N., C. K. Ghalambor, and K. Crooks. 2008. Experimental studies of evolution in guppies: a model for understanding the evolutionary consequences of predator removal in natural communities. *Molecular Ecology* 17:97–107.
- Rosenzweig, M. L., and R. H. MacArthur. 1963. Graphical representation and stability conditions of predator-prey interactions. *American Naturalist* 47:209–223.
- Saccheri, I., and I. Hanski. 2006. Natural selection and population dynamics. *Trends in Ecology & Evolution* 21:341–347.
- Sinervo, B., E. Svensson, and T. Comendant. 2000. Density cycles and an offspring quantity and quality game driven by natural selection. *Nature* 406:985–988.
- Swain, D. P., A. F. Sinclair, and J. M. Hanson. 2007. Evolutionary response to size-selective mortality in an exploited fish population. *Proceedings of the Royal Society B: Biological Sciences* 274:1015–1022.
- Tuda, M. 1998. Evolutionary character changes and population responses in an insect host-parasitoid experimental system. *Researches on Population Ecology* 40:293–299.
- Vos, M., B. W. Kooi, D. L. DeAngelis, and W. M. Mooij. 2004. Inducible defences and the paradox of enrichment. *Oikos* 105: 471–480.
- Webb, C. 2003. A complete classification of Darwinian extinction in ecological interactions. *American Naturalist* 161:181–205.
- Yoshida, T., S. P. Ellner, L. E. Jones, B. J. M. Bohannan, R. E. Lenski, and N. G. Hairston Jr. 2007. Cryptic population dynamics: rapid evolution masks trophic interactions. *PLoS Biology* 5:1–12.
- Yoshida, T., N. G. Hairston Jr., and S. P. Ellner. 2004. Evolutionary trade-off between defence against grazing and competitive ability in a simple unicellular alga. *Proceedings of the Royal Society B: Biological Sciences* 271:1947–1953.
- Yoshida, T., L. E. Jones, S. P. Ellner, G. F. Fussmann, and N. G. Hairston Jr. 2003. Rapid evolution drives ecological dynamics in a predator-prey system. *Nature* 424:303–306.

Associate Editor: Matt J. Keeling

Editor: Mark A. McPeck